Design of Hemispherical Compound Eye Acoustic Lens Consisting of Concave Meniscus

凹メニスカスで構成される半球殻複眼音響レンズの設計

Yuji Sato[1†], Tadashi Ebihara[1], Koichi Mizutani[1], and Naoto Wakatsuki[1]
([1]Univ. Tsukuba)
佐藤裕治 [1†]，海老原格 [1,2]，水谷孝一 [1,2]，若槻尚斗 [1,2] ([1] 筑波大院・シス情工，[2] 筑波大・シス情系)

1. Introduction

Recently, the cooperative use of multiple underwater vehicles has attracted attention for more efficient ocean exploration [1]. Underwater acoustic (UWA) communication is one of the techniques to establish underwater mobile network. However, the establishment of an UWA network is still challenging, since the collision of packets on a shared single channel can result in performance degradation. Thus, multiple access techniques (*e.g.*, time-, frequency-, code- or space-division multiplexing) or packet scheduling algorithms have been considered.

As an alternative, we have proposed a space-division multiplexing UWA communication system using acoustic lenses and mirrors. The use of acoustic lenses has the potential to realize a simple UWA network because it can transmit and receive multiple beams simultaneously without the need for complicated circuits. A compound eye acoustic lens with partitions has been found to be effective in realizing multi-user communication [2]. However, due to the complex shape of lens and the high underwater resistance, it was not suitable to be mounted on an AUV.

In this paper, we design a hemispherical compound eye lens combined with a concave meniscus lenses to simplify the shape and reduce the underwater resistance. The focusing performance of the single meniscus lens is evaluated by simulation in comparison with that of the aplanatic lens[3].

2. Design of Lens

Figure 1(a) shows a schematic view of a compound eye lens system consisting of 6 concave meniscus lenses. The dotted lines indicate the separation of each lens segment. One segment of the meniscus lens is shown in Fig. 1(b). The first surface of each meniscus lens is spherical with a radius of 400 mm. The second surface is aspherical to correct spherical aberration and is designed using an optimization technique. The aperture of second surface is larger than that of the first surface D because the incident rays are refracted in the diffusing direction. Refractive index n, thickness d, and focal length f are initially determined. The optical path length through the center of each lens, l_0,

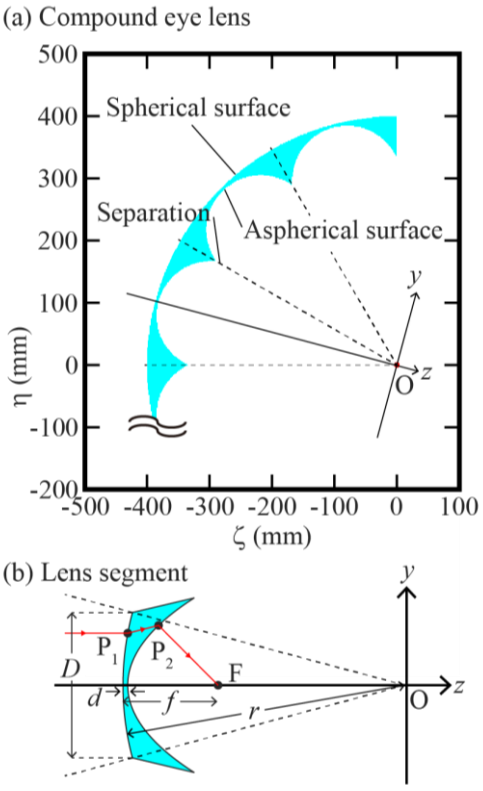

Fig. 1 Schematic view of lens; (a) compound eye lens and (b) lens segment.

is expressed as,

$$l_0 = nd + f - d. \quad (1)$$

The incidence point $P_1(z_1, y_1)$ is on the hemisphere and is expressed as,

$$z_1 = -r\cos(\alpha), \quad (2)$$

$$y_1 = r\sin(\alpha). \quad (3)$$

The refraction angle β on P_1 can be calculated by Snell's law as,

$$\beta = \sin^{-1}(\sin(\alpha) / n). \quad (4)$$

Therefore, the refracted acoustic ray can be expressed as,

$$y - y_1 = \tan(\beta - \alpha)(z - z_1). \quad (5)$$

The ray expressed by Eq. (5) is again refracted at the point $P_2(z_2, y_2)$ on the second surface. The ray then arrives at the focal point $F(f - r, 0)$. The optical path length of this ray, l, can be expressed as,

$$l = nP_1P_2 + P_2F. \quad (6)$$

The spherical aberration can be corrected when the

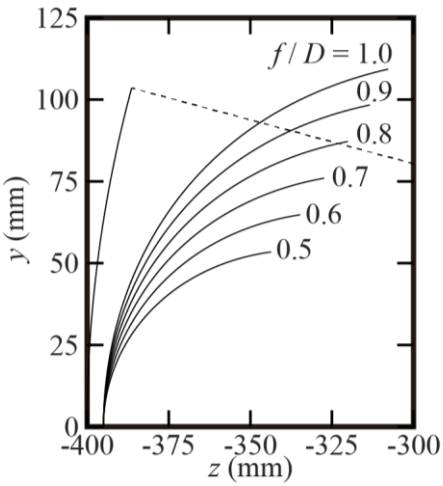

Fig. 2 Shapes of meniscus designed by several focal length f.

optical path lengths l is the same as l_0. However, it is difficult to analytically determine the position of P_2. Therefore, we change z_2 within a certain range to find the optical path length l that is closest to l_0. As long as $l = l_0$ holds, the calculation will be conducted sequentially from $y_1 = 0$ to $y_1 = D/2$. If $l = l_0$ does not hold, the calculation is terminated.

In addition to the number of meniscus lens and the radius of the spherical surface, we initially adopted the refractive index $n = 0.56$ and the thickness $d = 5$ mm in this design. Thus, the shape of the lens would depend on the focal length f. Several shapes of the lens are shown in **Fig. 2**. The focal length f was varied from $0.5D$ to $1.0D$ at intervals of $0.1D$. The dotted line indicates the separation line same as in Fig. 1(a). The longer the focal length f is, the larger the aperture of the second surface becomes because the calculation is continued under the condition $l = l_0$. Focal lengths $f = 0.5D$, $0.6D$ and $0.7D$ are not sufficient because their second surfaces does not cross the separation line, while the second surfaces of $f = 0.8D$, $0.9D$, and $1.0D$ cross the separation line. Therefore, we decided to use $f = 0.8D$ because interval between the lens and transducer becomes narrow.

3. Simulation

The focused sound pressure field was calculated using the 2-dimensional finite difference time domain (2D FDTD) method. In the simulation, a discretization steps of 0.25 μs and 1 mm in space were set. A chirp signal (center frequency: 37.5 kHz and bandwidth: 5 kHz) was emitted from the line source. The angle of incidence θ was varied from 0° to 15° at the intervals of 5°. For comparison, the pressure field of an aplanatic lens designed with the same aperture and focal length was also calculated.

The calculated focal areas are shown in **Fig. 3**. Here, the focal areas are defined as the area above

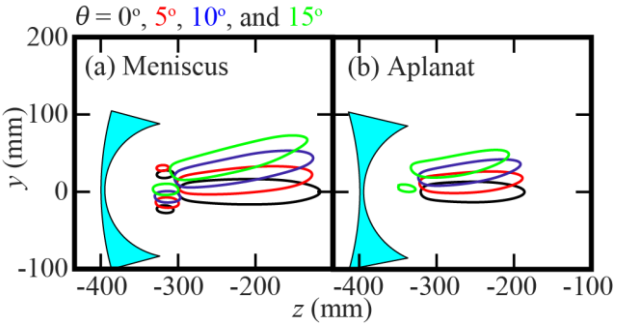

Fig. 3 Focal areas at changing angle of incidence θ; (a) meniscus and (b) aplanat.

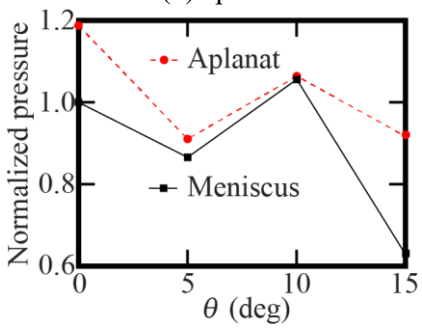

Fig. 4 Focal sound pressures at changing angle of incidence θ.

half of the maximum value of each incidence angle. Even if the angle of incidence θ changes, the shape of the focal area does not change significantly. The size of the focal area of the meniscus is larger than that of the aplanat. This is thought to be due to the difference in aberration correction capability.

The calculated focal pressures are shown in **Fig. 4**. The pressures are normalized by the focal pressure of the meniscus at angle of incidence $\theta = 0$. The aplanat shows higher pressure than the meniscus at all angle of incidences. The difference becomes large at $\theta = 15°$ because of the coma aberration, which can not be corrected by the meniscus.

4. Conclusions

In this paper, we designed a meniscus and evaluated its performance by simulation. As a result, we found the performance of the meniscus is lower than that of the aplanat, although the shape of the meniscus is suitable for mounting AUVs. In the future, we would like to clarify to what extent the degradation of focusing performance affects the communication performance.

Acknowledgment
This work was supported by JSPS KAKENHI Grant Number 19H02351.

References

1. Sozer *et al.*: IEEE J. Ocean. Eng., **25** (2000) 72.
2. Y. Sato *et al.*: Proc. USE2019 (2020) 1P6-2.
3. Y. Sato *et al.*: Jpn. J. Appl. Phys. **46** (2007) 4982.